

Stress Zones near Displacement Piers: II. Radial Cracking and Wedging

R. L. Handy¹ and David J. White²

Abstract: Transient liquefaction of saturated soils near Rammed Aggregate Piers is described in Part I on the basis of radial stress measurements. This is supported by dynamic pore-water pressure measurements, as peak pore pressures approximately equal radial stresses imposed at the pier surface by ramming. Stress measurements outside of the liquefied/plastic zone indicate radial tension cracking in the elastic zone, which is consistent with the observation that pore pressures abruptly drop and momentarily can even become negative as soon as ramming stops. The drainage field created by extended radial cracking and hydraulic fracturing allows Rammed Aggregate Piers to be effective in saturated, fine-grained soils where other dynamic methods are reported to be less effective. Stress measurements indicate that liquefied soil injected into open tension cracks causes stress to be retained in the elastic zone through arching action. A stress path analysis indicates that lateral stress may play an important role in control of foundation settlement, by simulating an increase in the preconsolidation pressure without vertically surcharging the soil or waiting for it to consolidate.

DOI: 10.1061/(ASCE)1090-0241(2006)132:1(63)

CE Database subject headings: Piers; Lateral stress; Pore water pressure; Liquefaction; Fractures; Cracking; Wedges.

Introduction

Rammed Aggregate Piers have been shown to be effective for reducing settlement of structures on soft, saturated, fine-grained soils where other dynamic methods such as vibro-compaction, heavy tamping, and blasting are reported to be less effective (Mitchell 1982). One assumption has been that excess pore water pressure is relieved into pore spaces in the aggregate. However, densely compacted, graded aggregate used in the piers has a relatively low porosity and permeability, and no water has been observed emerging from the piers either during or after their completion.

Part I of this two-part series presented evidence for temporary liquefaction of saturated soil close to the rammer, and subsequent drainage that reduces total stresses to effective stresses that are in accordance with predictions from plastic cavity expansion theory. Part II herein presents in situ stress measurements that indicate development of radial tension cracks in the elastic zone, and supplemental pore-water pressure measurements that confirm the transient nature of the liquefaction and indicate that water is conducted away from the adjacent plastic zone as it is being compacted during ramming of subsequent aggregate layers.

Previous Studies of Radial Cracking

Radial cracking has long been suspected as playing a role in the observed rapid dissipation of excess pore water pressures from fine-grained soils adjacent to driven displacement piles. Massarch (1978) presented an analysis based on cavity expansion theory that indicates that the stress and pore pressure conditions may allow radial hydraulic fracturing in the plastic zone, and he predicted an array of vertical fractures with a length of 1.5–2.2 m. In their discussion to Massarch's paper, Carter and Randolph (1979) acknowledged that while radial cracks must exist in order to explain the observed rapid reduction of pore-water pressure, they are unlikely to survive remodeling in the plastic zone and therefore should occur at "intermediate radial distances," presumably by extending into the elastic zone.

The present paper approaches the problem by means of radial stress measurements made in situ at varying distances and depths from rammed aggregate displacement piers.

Theory

Radial Stress around Expanding Cylinder in Elastic Zone

Cavity expansion theory indicates that with increasing radial distance from an expanding cylinder, plastic conditions give way to an elastic response mechanism (Vesic 1972; Baguelin et al. 1978). The elastic case is described by the Lamé solution, which can be written with an infinite external radius to define radial stress in an infinite elastic medium around an expanding cylindrical element

$$\sigma'_r = \sigma'_h + (\sigma'_{if} - \sigma'_h)[r_f/r]^2 \quad (1)$$

where σ'_r = radial effective stress at radial distance r from the center of the element; σ'_h = external or field stress; and σ'_{if} = radial stress at the element radius r_f . The equation is adapted to cavity expansion theory by considering the expanding element to be the

¹Distinguished Professor Emeritus, Dept. of Civil, Construction, and Environmental Engineering, Iowa State Univ., Ames, IA 50011-3232 (corresponding author). E-mail: rlhandy@iowatelecom.net

²Assistant Professor, Dept. of Civil, Construction, and Environmental Engineering, Iowa State Univ., Ames, IA 50011-3232.

Note. Discussion open until June 1, 2006. Separate discussions must be submitted for individual papers. To extend the closing date by one month, a written request must be filed with the ASCE Managing Editor. The manuscript for this paper was submitted for review and possible publication on August 24, 2004; approved on June 9, 2005. This paper is part of the *Journal of Geotechnical and Geoenvironmental Engineering*, Vol. 132, No. 1, January 1, 2006. ©ASCE, ISSN 1090-0241/2006/1-63-71/\$25.00.

outer boundary of the plastic zone of radius r_f . Rearranging and taking the logarithm

$$\log(\sigma'_r - \sigma'_h) = [\log(\sigma'_{rf} - \sigma'_h) + 2 \log r_f] - 2 \log r \quad (2)$$

As the term in the square brackets is constant, this is a linear equation in the form $y=a+bx$ with the slope $b=-2$. Data that are in agreement with this equation therefore should plot as a straight line on logarithmic axes with a slope of -2 . It is noted that the y axis term represents the increase of radial stress over the pre-existing lateral in situ stress, and not the total radial stress.

Tangential Stress in Elastic Zone

Elastic Theory

As radial stress increases inside a circular hole in an elastic medium, tangential stress decreases by the same amount at radial distance, r . Eq. (1) is modified by changing a sign as follows

$$\sigma'_t = \sigma'_h - (\sigma'_{rf} - \sigma'_h)[r_f/r]^2 \quad (3)$$

where σ'_t = tangential effective stress and other symbols are as previously defined. With an interior plastic zone tangential stress will be a minimum at the boundary between the plastic and elastic zones where $r=r_f$, and

$$\sigma'_t = 2\sigma'_h - \sigma'_{rf} \quad (4)$$

From Eq. (4), tangential stress becomes negative when radial stress σ'_{rf} at the contact with the plastic zone exceeds two times the field stress σ_h . As soil is weak in tension, this introduces a potential for radial tension cracking.

Stress Concentration Factor

Stress that is transferred through grain-to-grain contacts is not uniformly distributed, but is concentrated in some areas and diminished in others. The ratio of the maximum to the average stress is defined as a stress concentration factor. The theoretical factor for an elastic material around a circular hole is 3, in effect reducing the stress required for tension cracking by a factor of 3 (Murphy 1946). The factor is orders of magnitude higher at the ends of cracks, and a common method for preventing crack extension in a brittle material such as glass is to drill a small hole at the end to reduce the factor to 3.

Radial tension cracking therefore is almost a certainty in an elastically responsive soil if the average radial compressive exceeds two times the field horizontal stress, and because of stress concentration is likely to occur where the average radial stress is only marginally higher than the field horizontal stress.

Modification of Elastic Stress Field by Radial Tension Cracking

Without a tangential restraint, the distribution of radial stress in the elastic zone becomes a simple problem in statics: In Fig. 1 if the radial contact pressure σ'_{rf} acts on area A_1 at radius r_f , and σ'_r is the radial stress on area A at radius r , equating forces in a radial direction gives

$$\sigma'_{rf}A_1 = \sigma'_rA \quad (5)$$

from which

$$\sigma'_{rf}r_f = \sigma'_r r$$

$$\sigma'_r = (\sigma'_{rf}r_f)/r \quad (6)$$

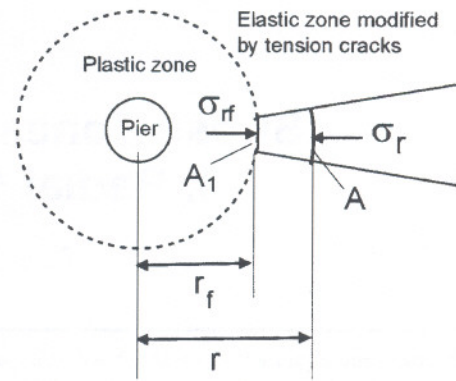


Fig. 1. Analysis of radial stress with zero tangential stress because of radial tension cracks

Expressed in logarithms, Eq. (6) becomes

$$\log \sigma'_r = [\log(\sigma'_{rf}r_f)] - \log r \quad (7)$$

where the term in the square brackets is constant. Data that are consistent with this equation therefore should plot as a straight line on logarithmic scales with a slope equal to -1 . The distinction between unmodified and crack-modified elastic behavior is illustrated in Fig. 2. It will be noted that Eq. (7) for the modified condition involves total radial effective stress, not an increase in radial stress as in the ideal elastic case.

Elastic Zone at Memphis, Tenn. Test Site

The methods used for measuring lateral stress with the K_0 stepped blade and for defining ranges and modes in test data are described in Part I of this two-part series. Soil properties at the test sites are presented in Table 1 of that paper.

Figs. 3–5 show test results at 2, 3, and 4 m depth at the Memphis, Tenn. site. Portions of these graphs were presented in Part I of this series. The arrows at the right indicate modes and ranges of lateral stresses measured prior to installation of the pier.

Criterion for Initiation of Elastic Radial Tension Cracking

The maximum stresses available to cause tension cracking are those at the outer margin of the plastic zone while it was liquefied. As shown in Figs. 3–5, peak stresses at the zonal boundary all exceed the field in situ stresses shown at the right in the graphs, and at the two deeper depths approach two times the field stresses (marked $\times 2$), indicating a high likelihood of tension cracking in the elastic zone.

Slope of Logarithmic Stress-Distance Curves

The $1:-1$ linear logarithmic relationship between radial stress and distance indicating radial tension cracking is shown at all three depths depicted in Figs. 4 and 5. Graphs of the data plotted according to elastic theory without tension cracks are curved and do not show that required constant slope of $1:-2$. The distribution of radial stress with distance therefore appears to confirm the existence of vertically oriented radial tension cracks in the elastic zone.

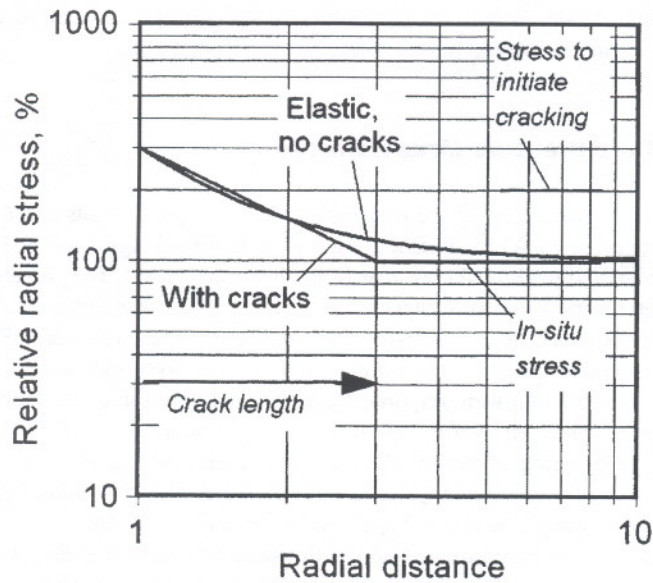


Fig. 2. Theoretical distribution of radial stress in elastic zone around displacement pier with and without radial tension cracks

Stress Retention in Elastic Zone

A zone of high radial stress in the elastic zone surrounding a zone of lower stress in the plastic zone is statically impermissible unless there is a contribution from arching action. Arching can occur if temporarily liquefied soil is pressure injected into open tension cracks during ramming, such that the injected soil solidifies into wedges that prevent the cracks from closing. A similar process is used in the petroleum production industry where sand is injected during hydraulic fracturing to keep radial cracks open for flow of petroleum into wells.

Stress Relief in Elastic Zone

Also of interest is that with increasing radial distance, the radial stresses shown in Figs. 3 and 5 diminish until they are lower than

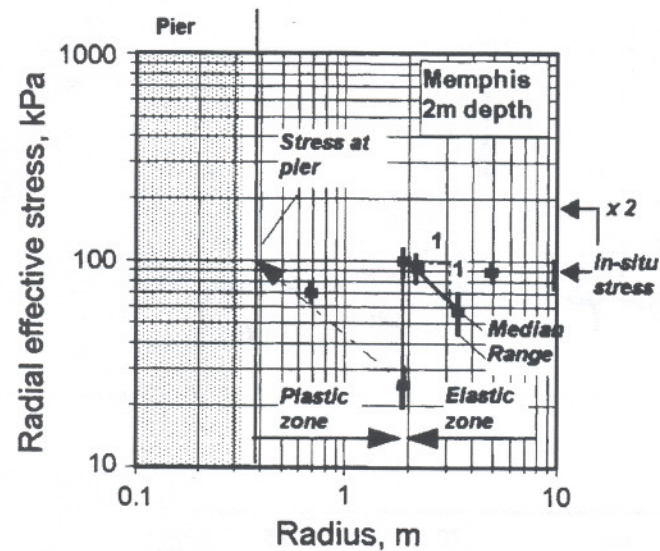


Fig. 3. Median radial stresses and ranges in stresses at 2 m depth at Memphis test site

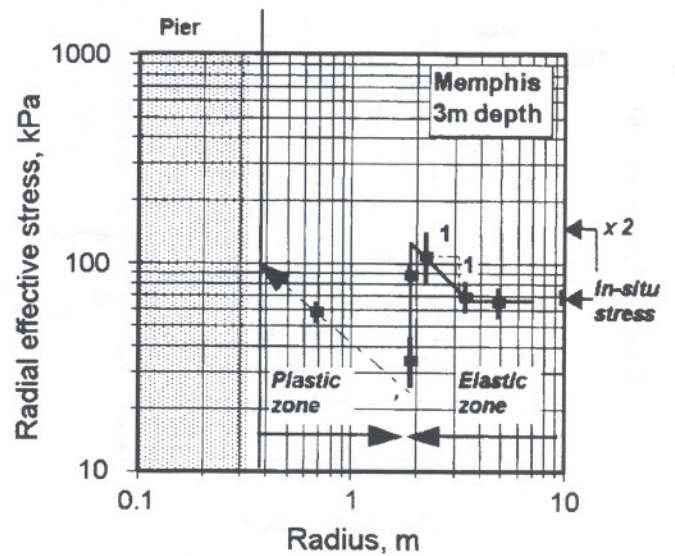


Fig. 4. Median radial stresses and ranges in stresses at 3 m depth at Memphis test site

the field stresses. This can be explained if injected material is concentrated at entrances to the cracks, reducing stresses in more distant regions.

Crack Length

As previously discussed, stress concentration factors related to the existence of voids in a particulate material can be expected to extend cracks until radial stress equals the field stress, and the cracks may extend farther if fluid pressure acts to open existing cracks. Minimum estimates for crack length can be obtained from end points of the sloping lines in Figs. 3–5. These end points indicate crack lengths extending 3.4–5 m (11–16 ft), being shortest at the shallower depth that is above the groundwater table, but still probably in a zone of capillary saturation.

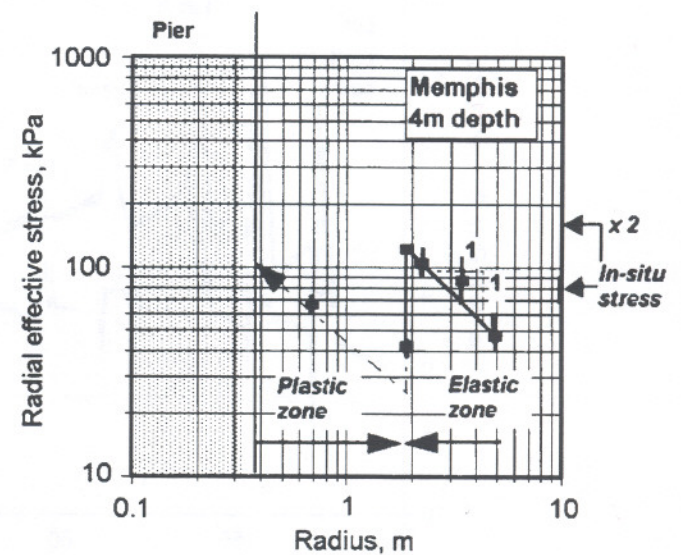


Fig. 5. Median radial stresses and ranges in stresses at 4 m depth at Memphis test site

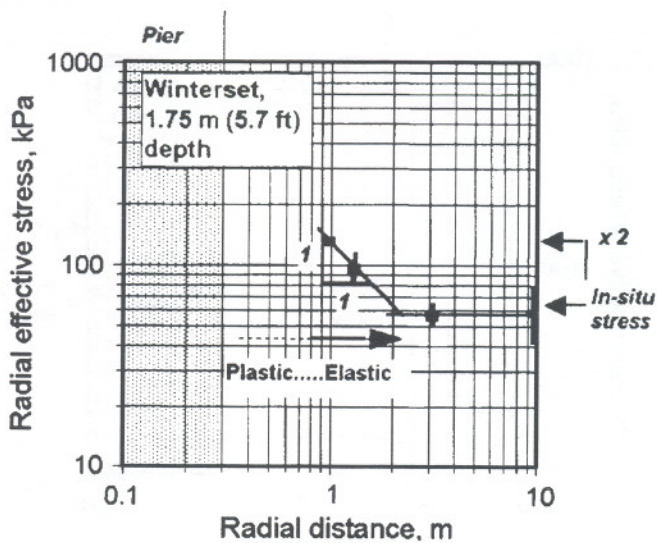


Fig. 6. Radial stresses measured in soil below 1.22 m pier depth at Winterset test site

Elastic Zone at Winterset, Iowa Test Site

Stress modes and ranges at a depth of 1.75 m in the soft, saturated loess at the Winterset test site are shown in Fig. 6. Tests were not conducted close enough to the pier to define a plastic zone. The 1:–1 slope in the elastic zone again indicates radial tension cracking, with an indicated crack length of 2 m measured from the center of the pier, which was confirmed by field observations. This length is shorter than at the Memphis, Tenn. site, probably the result of a smaller pier diameter and the use of a lower energy rammer. Arrows at the right in the figure show the field stress and 2× the field stress, and support the interpretation of tension cracking. As shown in Table 1 of Part I, moisture contents at the

test depths at both the Memphis and Winterset sites were at or slightly above the plastic limit.

Pore Pressure Measurements

As a further test of the drainage hypothesis, pore pressures were measured 0.43 m from the edge of a Rammed Aggregate Piers installed in alluvial clay near Neola in western Iowa. The piezometer boring logs indicated 5.1 m of redeposited or secondary CL loess over 1 m of water-bearing sand, over weathered shale. Piezocone data from the bottom of the sand layer indicated that about 6.7 min were required for a 50% reduction in excess pore-water pressure after a peak reading was obtained.

Geysering occurred when the piezometer boring entered the sand, indicating an artesian condition. Water also rose in the first pier boring as it penetrated the sand, so borings for other piers in the group were stopped above the sand and remained dry. The piezometers were monitored during ramming of the first pier.

Piezometer data are shown in Fig. 7. The upper lines show data at 4.9 and 6.1 m depths, which were in the alluvial silty clay and underlying sand, respectively. These pressures are nearly identical and indicate that each filling-and-ramming cycle required about 2 min, of which approximately 30 s were spent ramming. About 25 min were required for compaction of the entire pier.

During ramming, the pore pressure suddenly increased as much as 22 kPa in the lower piezometers and reached a maximum of 90 kPa. Pore pressures then precipitously declined when ramming stopped and momentarily became negative, indicative of rebound. They then almost immediately recovered, became positive, and showed a more gradual decrease prior to the next ramming.

The peak pore pressure is about 90% of the maximum lateral pressure typically developed during pier ramming, shown in

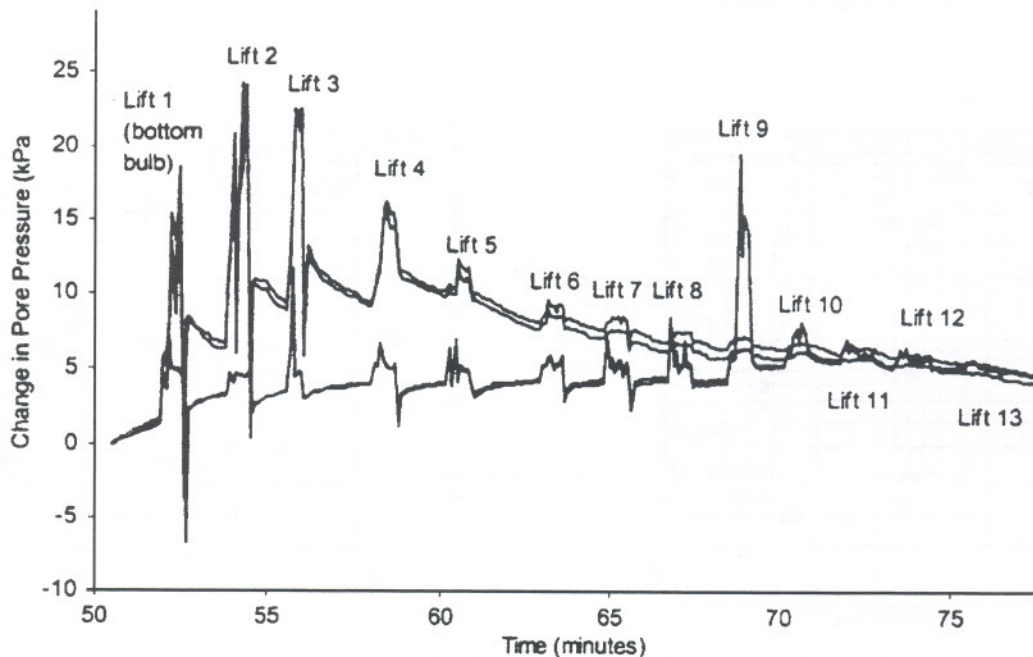


Fig. 7. Increased pore pressures measured during pier ramming in alluvial silty clay

Figs. 3–5. This is consistent with the interpretation of liquefaction during ramming.

The abrupt drop in pore pressure when ramming stops may be compared with the much longer time measured in the piezocone tests, and is attributed to drainage through radial tension cracks. Another possibility might be drainage through the underlying sand, but piezometers located at depths of 0.9 and 2.4 m show the same sudden drops in pore pressure when ramming stops, indicated by the lower lines in Fig. 7. The peak pressure measured during compaction of Lift 9 reflects its proximity to the upper two piezometers.

The transition to more gradual declines in pore-water pressure may be attributed to cracks becoming filled near their entrances by liquefied soil. Hydraulic pressure built up during subsequent ramming cycles tended to reopen the cracks and reactivate drainage.

Changes in pore pressure mainly occur during the first through the third cycles of ramming following installation of a particular layer. As ramming becomes more remote from the piezometers, negative pressures no longer occur, and the increase in pore pressure from ramming diminishes. Compaction of soil in the plastic zone therefore mainly occurs during ramming of the next one or two lifts. Peak pore pressures during ramming of the first lift were lower because that lift is composed of open-graded stone.

The final pore pressure is about 5 kPa higher than the initial pressure, which is attributed to tapping into the partially relieved artesian pressure in the sand.

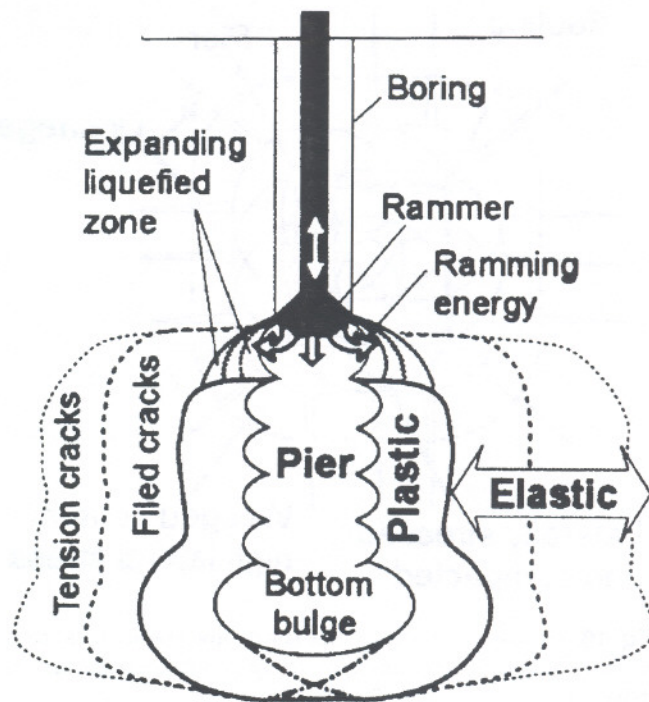


Fig. 8. Hypothesized zones developed during ramming of pier in soil below groundwater table. Liquefaction contributes to expanded plastic zone, and drainage occurs in tension cracks in the elastic zone.

Stress Sequence in Elastic Zone

Horizontal stresses in the elastic zone appears to evolve as follows:

1. The initial K_0 state is $K_a < K_0 < K_p$.
2. Ramming initially creates an elastic response, increasing the radial stress.
3. If radial stress exceeds the pre-existing K_0 stress, radial tension cracks reduce tangential stress to zero and create an inverse relationship between total radial effective stress and distance.
4. Radial cracks developing in saturated conditions form drainage paths for water ejected from compaction of the adjacent plastic zone, leading to a further extension of radial cracks by hydraulic fracturing.
5. Cracks are literally an open invitation for entry of temporarily liquefied soil from the adjacent plastic zone. When solidified, the injected soil forms wedges that preserve high stress near the inner boundary of the elastic zone while reducing it outside of that area. This should have little effect on foundation loads that normally are applied closer to the piers.
6. Liquefaction lasts as long as a ramming cycle, after which pore pressures are relieved in a matter of seconds.

A schematic diagram illustrating the different stages is shown in Fig. 9. Mitchell (1982) reports that 20% combined silt and clay is considered an upper limit for vibratory compaction to be effective. The soils in this investigation all exceed that content, the loessial soils being over 98% combined silt and clay. The performance of the piers equaled or exceeded design expectations, which emphasizes the importance of radial tension cracking to accommodate excess pore water ejected from soil during ramming compaction of a pier or pier group.

A three-dimensional representation of a single pier in uniform soil is shown in Fig. 9, which also shows necking in of the plastic zone above the level of capillary saturation. At shallow depth, passive failure will prevent full development of lateral stress from ramming, which in turn will tend to concentrate bulging in the upper part of the pier when the pier is loaded. This is supported

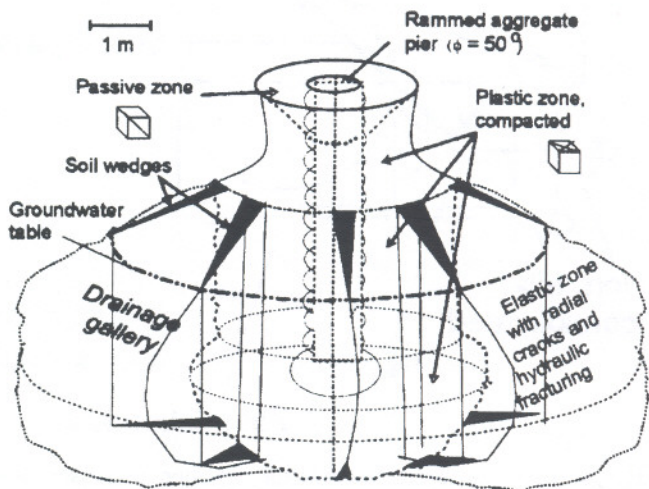
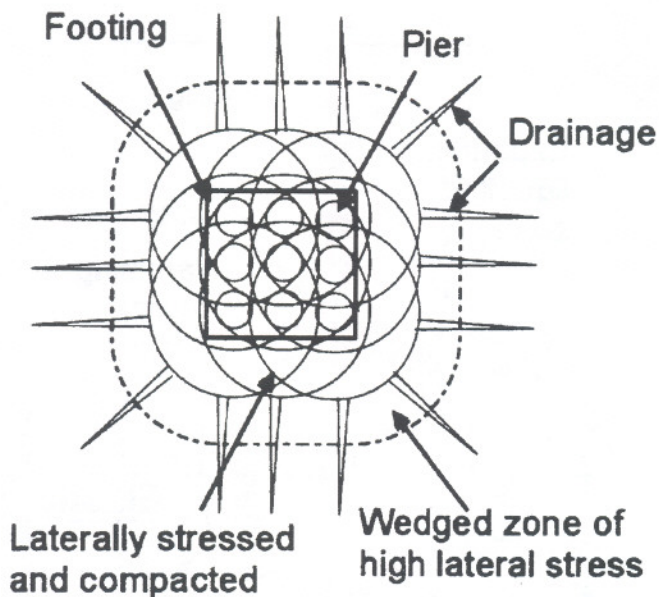


Fig. 9. Schematic representation of stress zones around single rammed aggregate pier



tions of the piers. Fig. 10 shows zone overlapping in a nine-pier group based on the Memphis model with a square footing dimension of 3.4 m (11.25 ft). The group is enclosed by a compacted and laterally stressed inner zone and an outer zone of higher stress resulting from wedging of soil in open cracks.

Installation Sequence

In order to assure drainage, pier groups should be installed as a progression without closure, which is the opposite of the procedure conventionally used in grouting. This sequence was adopted automatically when it was discovered that boring a hole can be very difficult in soil that is confined and compacted from all quarters by Rammed Aggregate Piers.

There's Mohr?

A stress path analysis indicated that a high lateral stress may replicate the influence of a preconsolidation pressure without actually preconsolidating the soil (Handy 2001). That development did not consider the intermediate principal stress; however, overlapping stress zones that do not affect the major principal stress do tend to increase the intermediate principal stress in the plastic zone, as discussed with regard to data presented in Fig. 9 of Part I.

The hypothesis regarding a simulated preconsolidation stress can be summarized as follows: At the left in Fig. 11 is a Mohr circle for a normally consolidated soil. If the minor principal stress remains constant, ramming can increase lateral stress up to a passive limit indicated by the second Mohr circle, or, if the minor principal stress also increases, as in a plastic zone, the second circle moves farther to the right. Application of a vertical foundation load then can increase vertical stress to a limit defined by the third Mohr circle before initiating consolidation settlement. A naturally overconsolidated soil will move the first circle to the right as far as the second circle, but does not change the geometry of the third circle. The stress-induced increase in preconsolidation pressure appears to be accompanied by an increase in modulus (White and Pham, private communication 2005). This analysis supports the current settlement design for soil reinforced by Rammed Aggregate Piers, which assumes elastic response in the zone penetrated or affected by the piers, and normal consolidation in soil below that zone.

Relief of Lateral Stress

Consolidation that is prevented by a high lateral stress presumably could begin if lateral stress is removed, as by trenching. Acting to prevent this is a tendency for remolded soil to gain strength in time. This is revealed by a "setup factor" for driven pile. Laboratory tests indicated a time-related increase in preconsolidation pressure, with the result that a truly normally consolidated soil can be a laboratory oddity that is rare in nature (Schmertmann 1991). Time-related strength gains occur even in sands, attributed to an increase in friction and dilatancy. If friction

Fig. 10. Hypothesized stress zones below groundwater table around rammed aggregate piers. Similar behavior on smaller scale can occur above gwt.

by load tests using telltales installed in the piers (Lawton and Merry 2000).

Pier Groups

The radial extent of the plastic zone and of tension cracking assume added significance in pier groups where the zones overlap. Limited measurements of lateral stress within pier groups indicate uniform stress that is multidirectional and not related to the posi-

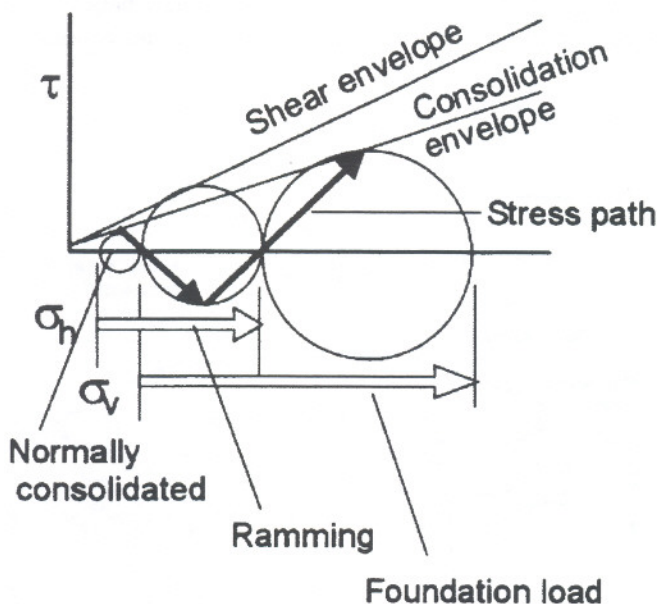


Fig. 11. Hypothesized mechanism for reduction of consolidation settlement by increasing lateral soil pressure. Arrow labeled "Ramming" shows maximum increase in simulated preconsolidation pressure that also may influence modulus [adapted from Handy (2001)].

involves contact bonding this may reflect an equalization of intergranular contact stresses as weak bonds become stronger and strong bonds become weaker, with slippage depending on a summation of strengths along selected weaker contacts. Nevertheless, relief of lateral stress should be avoided during and immediately after pier installation to allow time for the soil to gain sufficient strength to remain stable.

Conclusions

In situ stresses measured in soil near Rammed Aggregate Piers appear to conform to the conventional concept of a remolded, plastic zone surrounded by an elastic zone, but with some important modifications. The following conclusions embody results from both Part I and Part II of the investigation:

1. Radial tension cracking occurs if radial stress induced by ramming is about two times the pre-existing field stress, and is likely to occur if it exceeds the field stress. This can occur in unsaturated as well as in saturated soil.
2. In saturated soil or soil that becomes saturated during ramming, temporary liquefaction acts to transfer ramming stress outward, enlarging the liquefied zone and increasing the extent of radial cracking. The liquefied zone will continue to expand as long as ramming continues and liquefied soil pressures exceed the compressive strength of the soil.
3. Open cracks form a drainage gallery for water ejected as soil in the liquefied zone compacts and becomes plastic. This allows the system to be effective in fine-grained soils.
4. Liquefied soil injected into open tension cracks creates soil wedges that preserve radial and tangential stress in the elastic zone.
5. Liquefaction is transient, as drainage occurs in a matter of seconds after ramming stops on each layer in the pier. Compaction of soil in the liquefied zone therefore is essentially complete after ramming of the next two or three layers of a pier.
6. Compaction in layers from the bottom up normally creates a containment for liquefied soil, but soil also can be displaced laterally and replaced by aggregate where ramming encounters very soft soil layers.

These conclusions may be modified as stress measurements are made near piers installed in a wider variety of soils. It also can be anticipated that observations made in these studies may also apply to other dynamic displacement elements such as driven pile.

The system is far more complex than previously imagined.

Acknowledgments

More detailed acknowledgements are included in Part I of this series. Cone data and interpretations were by Geotechnical Services, Inc., Omaha, with Steven Saye the senior engineer. Pore-pressure measurements were made as part of a research project at the Spangler Geotechnical Laboratory of Iowa State University, sponsored by the Iowa DOT. The investigation demonstrates the complementary relationship between theory, measurements, and models, and suggests the limitations that would derive from a dependence on one of these approaches without the others. The

writers gratefully acknowledge the contributions of many students and colleagues who were involved at one time or another in the research and discussions. The writers serve as research consultants for Geopier, a subsidiary of the Tensar Corporation.

Appendix. Lateral Stresses Measured In Situ at Four Test Sites

Site	Boring and radial distance (m)	Depth (m)	Stress (kPa)	Effective stress (kPa)	
Memphis Tenn. (loess)	B-1	1.56	83	83	
		0.00	97	97	
		(K_o)	182	112	
			265	72	
			278	62	
			357	72	
			370	71	
	B-4	1.44	45	45	
		1.90	156	21	
			169	97	
			182	34	
			265	32	
			278	19	
B-5	1.90	2.91	39	39	
		3.04	46	46	
		3.57	52	48	
		3.70	52	47	
		3.82	52	46	
		3.95	48	41	
			144	84	84
			156	111	111
			169	92	92
			182	119	119
B-3	2.21	2.65	81	79	
		2.78	89	85	
		2.91	99	94	
		3.04	92	86	
		3.87	63	48	
		4.00	134	119	
		4.13	148	130	
			144	73	73
	156	48	48		
	169	66	57		
	250	85	82		
	263	138	134		
	276	90	85		
	288	174	168		
	479	138	113		

References

- Baguelin, F., Jézéquel, J. F., and Shields, D. H. (1978). *The pressuremeter and foundation engineering*, Trans Tech Publications, Clasuthal, Germany.
- Carter, J. P., and Randolph, M. F. (1979). "Discussion of 'New aspects of soil fracturing in clay' by K. Massarch." *J. Geotech. Eng. Div., Am. Soc. Civ. Eng.*, 105(8), 993–995.
- Handy, R. L. (2001). "Does lateral stress really control settlement?" *J. Geotech. Geoenviron. Eng.*, 127(7), 623–626.
- Lawton, E. C., and Merry, S. M. (2000). "Performance of Geopier-supported foundations during simulated seismic tests on northbound Interstate 15 Bridge over South Temple, Salt Lake City, Utah." *Rep. No. UUCVEEN 00-03*, Dept. of Civil and Environmental Engineering, Univ. of Utah, Salt Lake City, Utah.
- Massarch, K. R. (1978). "New aspects of soil fracturing in clay." *J. Geotech. Eng. Div., Am. Soc. Civ. Eng.*, 104(8), 1109–1123.
- Mitchell, J. K. (1982). "Soil improvement—State of the art report." *Proc., 10th Int. Conf. on Soil Mechanics and Foundation Engineering*, Vol. 4, A. A. Balkema, Rotterdam, The Netherlands, 509–566.
- Murphy, G. (1946). *Advanced mechanics of materials*, McGraw-Hill, New York.
- Schmertmann, J. (1991). "The mechanical aging of soils." *J. Geotech. Eng.*, 117(9), 1288–1330.
- Vesić, A. S. (1972). "Expansion of cavities in infinite soil mass." *J. Soil Mech. Found. Div.*, 98(3), 265–290.

Site	Boring and radial distance (m)	Depth (m)	Stress (kPa)	Effective stress (kPa)
		3.54	44	27
		3.67	53	35
		4.46	45	19
		4.58	39	12
Des Moines, Iowa	B-1 and B-2	0.99	—	—
	0.85	1.09	55	65
			81	88
(glacial till)		1.19	74	79
		1.30	91	108
		1.91	—	79
		1.96	66	—
		2.01	—	116
		2.06	83	—
		2.11	—	108
		2.17	135	—
		2.82	112	65
		2.92	102	108
		3.02	81	84
		3.12	—	85
		3.73	—	91
		3.83	—	94
		3.94	—	139
		4.04	109	—
		4.24	130	—

^aTotal stress.